Earth and Planetary Science Letters 301 (2011) 231–240

Contents lists available at ScienceDirect

Earth and Planetary Science Letters

journal homepage: www.elsevier.com/locate/epsl

Cooling-induced fractionation of mantle Li isotopes from the ultraslow-spreading Gakkel Ridge

Yongjun Gao [a,*], Jonathan E. Snow [a], John F. Casey [a], Junbao Yu [b]

[a] Department of Earth and Atmospheric Sciences, University of Houston, Houston TX, 77204, USA
[b] Laboratory of Coastal Wetland Ecology, Key Laboratory of Coastal Environment Processes, Yantai Institute of Coastal Zone Research, Chinese Academy of Sciences, Yantai, 264003, PR China

ARTICLE INFO

Article history:
Received 11 June 2010
Received in revised form 26 October 2010
Accepted 1 November 2010
Available online 26 November 2010

Editor: R.W. Carlson

Keywords:
Li isotopes
diffusion
isotope fractionation
modelling
upper mantle

ABSTRACT

Li isotopic compositions of magmatic rocks have gained considerable attention recently as probes of mantle-scale processes. However, the concentrations and isotopic composition of Li in mantle minerals from mid-ocean ridges remain relatively unconstrained. This is largely because of the general presence of seawater alteration in abyssal peridotites. Lithium elemental and isotopic compositions for mineral separates of coexisting olivine, clinopyroxene, orthopyroxene and bulk rocks of serpentine-free Gakkel Ridge peridotites were investigated. Bulk rocks have Li contents of 1.6 to 2.7 ppm and δ^7Li values of 3 to 5‰, which fall within the range of reported normal pristine "MORB mantle" values. Lithium concentrations vary in the order cpx (2.1–4.7 ppm) > opx (0.9–1.7 ppm) ≥ olivine (0.4–0.9 ppm), the opposite found in "equilibrated" mantle peridotite xenoliths (Seitz and Woodland, 2000). The Li isotopic compositions indicate a systematic mineral variation with $\delta^7Li_{olivine}$ (7.14‰–15.09‰) > δ^7Li_{opx} (1.81‰–3.66‰) > δ^7Li_{cpx} (−2.43‰ − −0.39‰). The δ^7Li values of cpx are negatively correlated with their Li concentrations with the lightest value for the most enriched cpx grains. There is a first order negative linear correlation between $\Delta_{olivine-cpx}$ ($\delta^7Li_{olivine} - \delta^7Li_{cpx}$) and $^{ol/cpx}D$ ($Li_{olivine}/Li_{cpx}$).

Numerical simulations indicate that the observed systematic inter-mineral variations of Li concentrations and isotopic compositions could be explained by a cooling driven diffusive redistribution between minerals in a closed system if there is a temperature dependent partitioning of Li between olivine and clinopyroxene. The studied Gakkel Ridge abyssal peridotites may alternatively have cooled under a variable cooling rate with a rapid cooling before the Li system was closed, which is less likely given the tectonic setting. Our calculations confirm that Li systematics in minerals, especially in coexisting mineral phases could potentially be used as a mantle geospeedometer, even for slowly cooled mantle rocks.

Published by Elsevier B.V.

1. Introduction

The utility of Li isotopes stems from the very large mass fractionation that can occur in natural processes, where up to 80‰ variation of ^{7}Li/^{6}Li has now been documented in terrestrial samples (Rudnick and Nakamura, 2004). In addition to the intrinsically large fractionations observed for ^{7}Li/^{6}Li, other properties, such as the single valence state and the affinity of Li for fluids, make it a potentially unique tracer for fluid–rock interaction in the Earth (Elliott et al., 2004; Tomascak, 2004). Lithium is moderately incompatible during mantle melting (Brenan et al., 1998a; Ryan and Langmuir, 1987) and is strongly fluid-mobile (e.g. Brenan et al., 1998b; Seyfried et al., 1984, 1998; Zack et al., 2003). During water–rock interaction Li may be leached out from the solid phases into aqueous solutions or be incorporated from aqueous solutions to the newly formed secondary minerals, depending on the temperature (Berger et al., 1987, 1988; James et al., 2003). The large fractionation of ^{7}Li and ^{6}Li between solid and aqueous phases during near-surface alteration process as well as metamorphic dehydration in subduction zones make the Li-isotope system a potentially powerful tracer of crust–mantle recycling (e.g. Elliott et al., 2004, 2006; Leeman et al., 2004; Teng et al., 2004; Tomascak, 2004; Zack et al., 2003). In contrast to the proposed large and homogeneous reservoirs in the mantle with δ^7Li approximately + 4‰ (Ryan and Kyle, 2004; Tomascak et al., 2002), materials entering subduction zones (sediments and basaltic oceanic crust) have highly variable Li concentration and δ^7Li compositions ranging from +1.5‰ to +5.6‰ in fresh MORBs (Tomascak et al., 2008), −1.7‰ to +14‰ in altered basalts (Chan et al., 2002), and −0.4‰ to +9‰ in subducted sediments (Bouman et al., 2004; Chan et al., 2006). During subduction, the slab tends to be depleted in ^{7}Li (−11‰ to +5‰) due to the dehydration release of H_2O (Zack et al., 2003). Thus, the isotopic composition of the upper mantle with contributions of recycled components by subduction remains speculative, depending on the

* Corresponding author.
E-mail address: ygao@mail.uh.edu (Y. Gao).

0012-821X/$ – see front matter. Published by Elsevier B.V.
doi:10.1016/j.epsl.2010.11.003

dominant type of recycled materials (i.e. dehydrated slab versus sediment/subduction related fluids).

^{6}Li is predicted to diffuse about 2–3% faster than ^{7}Li based on their 16% mass difference (Lundstrom et al., 2005; Richter et al., 2003), which could act as an important process to generate Li isotopic variability at high temperatures. Diffusive Li-isotope fractionations have been broadly recognized in nature from meter scale to microns (Jeffcoate et al., 2007; Lundstrom et al., 2005; Marschall et al., 2007a, b; Parkinson et al., 2007; Teng et al., 2006). The elemental and isotopic disequilibrium of Li in minerals from peridotite xenoliths have been attributed to diffusion-controlled interaction with Li bearing fluids (Jeffcoate et al., 2007; Magna et al., 2008; Rudnick and Ionov, 2007; Tang et al., 2007). Ionov and Seitz (2008) demonstrated that the anomalously low δ^7Li clinopyroxenes together with both Li elemental and isotopic disequilibria could be produced in xenoliths hosted in slowly cooled lava. Based on investigations of inter-mineral fractionation as well as numerical modeling, it has been argued that large Li isotopic fractionations could occur by cooling processes alone (Gallagher and Elliott, 2009; Ionov and Seitz, 2008; Jeffcoate et al., 2007; Parkinson et al., 2007).

The rapid diffusion rates make the Li system suitable for high-resolution geospeedometry in near-surface geological environments where more rapid cooling takes place (Beck et al., 2006; Coogan et al., 2005; Jeffcoate et al., 2007; Parkinson et al., 2007). In contrast to the generally fast cooling of mantle xenoliths, abyssal peridotites exposed at Mid-Ocean Ridges represent upper oceanic mantle that is slowly cooled during upwelling and tectonic exhumation to the surface under mid-ocean ridges. Thus, diffusive fractionation of Li in such abyssal peridotites would be expected to have homogenized due to its long cooling duration. Direct measurements of Li and its isotopes in abyssal peridotites recovered at mid-ocean ridges are scarce and have mostly been performed on serpentinized and hydrothermally altered samples (Brooker et al., 2004; Decitre et al., 2002). To date, serpentinization and weathering of oceanic mantle rocks has limited the information that can be derived regarding the pristine upper mantle Li systematics. Due to the fluid mobility/affinity of the Li and the significantly different isotopic composition between seawater (+31‰; Chan and Edmond, 1988; Jeffcoate et al., 2004) and normal upper mantle (+4±2‰; Chan et al., 1992, 2002; Jeffcoate et al., 2007; Tomascak and Langmuir, 1999), the Li elemental and isotopic compositions in previously reported oceanic peridotites are nearly always contaminated with seawater.

Unaltered peridotites were recovered from one location in the Arctic Ocean along Gakkel Ridge, which is an ultraslow-spreading ridge with relatively weak magmatic activity and inferred melting (Dick et al., 2003; Michael et al., 2003; Snow et al., 2007). Both fertile and refractory depleted mantle domains co-exist at Gakkel ridge as revealed by osmium isotope study (Liu et al., 2008). Thus these peridotites provide, at present, a unique opportunity to observe the primary Li systematics inherited from the upper oceanic mantle in a mid-ocean ridge setting. Here, we present the Li content and δ^7Li compositions of bulk rocks and their component minerals (olivine, clinopyroxene, and orthopyroxene) of these unaltered peridotites.

2. Geological setting and sample description

Gakkel Ridge extends over 1800 km across the Arctic Ocean from the northeastern corner of Greenland to the Laptev Shelf, representing the slowest-spreading end-member in the global mid-ocean ridge system (Michael et al., 2003). Peridotite samples were recovered primarily between 3°E and 30°E in the sparsely magmatic zone (SMZ) (Snow et al., 2007), where spreading was amagmatic, with mantle peridotites emplaced directly on the sea floor at the spreading axis (Michael et al., 2003).

Peridotite dredge haul PS66-238 was recovered at the western edge of SMZ during Expedition ARK XX-2 (Snow et al., 2007). The derdge included all major peridotite types (lherzolite, harzburgites, enstatite–dunite) except for orthopyroxene-free dunites (Liu et al., 2008; Von de Handt, 2008). The textures of peridotites studied range from coarse-granular to mildly porphyroclastic. Olivine grain size ranges up to 1 cm, whereas orthopyroxenes are disseminated grains to cm-scale porphyroclasts. Clinopyroxenes are mostly fine and disseminated grains in the matrix along grain boundaries of olivine and/or orthopyroxene. Serpentine fibers are not detectable in thin section. Olivine grains investigated by FTIR show no evidence of micro-inclusions of serpentine (Peslier et al., 2007). The only visible alteration present is a dun-colored rind around the margins of the sample that is typical of seafloor weathering. The rind was removed before powdering.

3. Analytical techniques

Minerals were first separated through a Frantz magnetic barrier separator from crushed rocks and then handpicked under a binocular microscope. Only those grains without any sign of alteration, cracks, and discoloration were picked for analysis. Mineral grains were washed in ultrasonic bath with Milli-Q water to remove any possible surface contamination. The mineral grains were not further leached with acid, as it has been reported that this treatment had little influence on measured results (Jeffcoate et al., 2007). All reagents used (HF, HNO_3, HCl) were double distilled and ultrapure 18.2 megaohm water was used. Pressure bombs from Parr Instruments were used to achieve complete digestion (Gao et al., 2009). A reflux procedure with HCl and HNO_3 was repeated 3–4 times to break down the insoluble fluoride for high-Mg and high-Ca samples. An aliquot of each sample solution was analyzed for Li concentration using a Varian 810 quadruple ICP-MS at University of Houston with a precision of 5.2% RSD monitored by repeated analysis of USGS standard DTS-2 and JP-1 (Gao and Casey, in press). The Li concentration in rock samples was also measured by voltage comparisons with that obtained for L-SVEC standard of known concentration and then adjusted for sample weight. The uncertainty in Li concentration determined by this method is better than ±10% (Teng et al., 2007).

Separation of Li for isotopic composition analysis was achieved by an organic solvent free two-step liquid chromatography procedure in a clean lab at the University of Houston following the procedure described by Gao and Casey (in press). To avoid the problems induced from the usage of organic solvent, such as the degradation of resin and the residue Ca in methanol, 0.2 N HCl was used in both first and second columns to elute Li (Gao and Casey, in press). All separations were monitored with ICP-MS analysis to guarantee both high Li yield (>99.8%) and low Na/Li ratio (<0.5). The high Li yield is also indicated by the good agreement of Li concentrations measured by ICP-MS and MC-ICP-MS (Table 1). Cation exchange columns were made of quartz glass with an internal diameter of 10 mm. They were filled with 15 mL wet Bio-Rad AG 50 W X-8 resin in H_2O (200–400 mesh) for first step columns and 5 mL wet Bio-Rad AG 50 W X-12 resin in H_2O (200–400 mesh) for second step columns. Large columns were used to ensure that the column was not saturated for sodium and other cations. This is important for low Li and/or high-Mg rocks and minerals. High-Mg samples tend to have more equivalent cations than those with high Fe content at a given weight. It has been suggested that good ion selectivity can only be effectively maintained for ion quantities that do not exceed 10% of the capacity of resin in term of milliequivalents (meq) (James and Palmer, 2000; Rieman and Walton, 1970). Given the capacity of 15 mL AG50-X8 resin of 25.5 meq and the equivalent weight for common silicate rock of about 55 mg/meq (exclude Si), our first step column could effectively treat sample sizes up to 130 mg.

The final concentrations of Li solution for MC-ICP-MS analysis are about 50 ppb to ensure the best precision and accuracy. The total procedure blanks determined for both the column procedure alone and the combined sample digestion and column procedure were

Table 1
Lithium concentrations and isotopic compositions of peridotites and its major component minerals from Gakkel Ridge.

Sample	Lithology	Phase	Mode (%)	Li (ppm)[a]	Li (ppm)[b]	δ^7Li ‰	Cal. Li (ppm)	Cal. δ^7Li
PS66-238-2	PL-LH	Cpx	8	2.32	2.09	−0.39		
		Opx	22	0.94	1.10	3.66		
		Ol	70	0.96	1.16	8.74		
		Bulk		1.55	1.46	3.57	1.06	6.16
PS-66-238-7	SP-LH	Cpx	8	3.88	3.85	−1.79		
		Opx	17	1.64	1.69	4.79		
		Ol	75	1.01	0.92	15.09		
		Bulk		1.72	1.70	3.77	1.34	9.06
PS66-238-9	PL-LH	Cpx	10	3.65	3.79	−1.76		
		Opx	20	1.70	1.75	1.81		
		Ol	70	1.16	1.26	14.26		
		Bulk		1.70	1.80	3.03	1.52	7.63
PS66-238-11	SP-LH	Cpx	11	3.11	3.14	−1.3		
		Opx	7	1.81	1.83	2.34		
		Ol	82	0.85	n.d.	n.d.		
		Bulk		2.85	2.70	4.34	1.17	
PS66-238-18	PL-LH	Cpx	15	3.67	3.75	−1.56		
		Opx	20	1.70	1.67	2.96		
		Ol	65	1.18	1.22	6.89		
		Bulk		1.54	1.44	3.14	1.66	3.27
PS66-238-22	SP-HZ	Cpx	3	1.99	1.94	−0.86		
		Opx	12	0.94	1.04	3.94		
		Ol	85	1.15	1.14	7.17		
		Bulk		1.47	1.42	3.98	1.15	6.43
PS66-238-35	SP-LH	Cpx	11	2.36	2.19	−1.13		
		Opx	14	1.33	1.23	1.89		
		Ol	75	0.93	1.15	8.38		
PS66-238-39	SP-LH	Cpx	12	2.40	1.95	−0.82		
		Opx	18	1.13	1.23	2.26		
		Ol	70	1.06	1.21	7.14		
		Bulk		1.55	1.48	3.19	1.23	4.47
PS66-238-49	PL-LH	Cpx	11	4.70	5.08	−2.43		
		Opx	9	1.20	1.16	2.38		
		Ol	80	0.64	0.66	12.81		
		Bulk		2.65	2.55	4.53	1.14	4.90

All samples were collected during ARK XX-2 expedition on 2004 (Snow et al., 2007). Mode compositions were visually estimated with onboard thin sections during the expedition assuming opx + cpx + ol = 100%. SP-LH = spinel Lherzolite; SP-HZ = spinel harzburgites; PL-LH = plagioclase lherzolite. cpx = clinopyroxene; opx = orthopyroxene; ol = olivine. Cal. Li (ppm), and Cal. δ^7Li are calculated bulk compositions based on mineral data and mode composition.

[a] Lithium measured by ICP-MS at University of Houston.

[b] Lithium measured by voltage comparison with 50 ppb L-SVEC with Nu Plasma at University of Maryland.

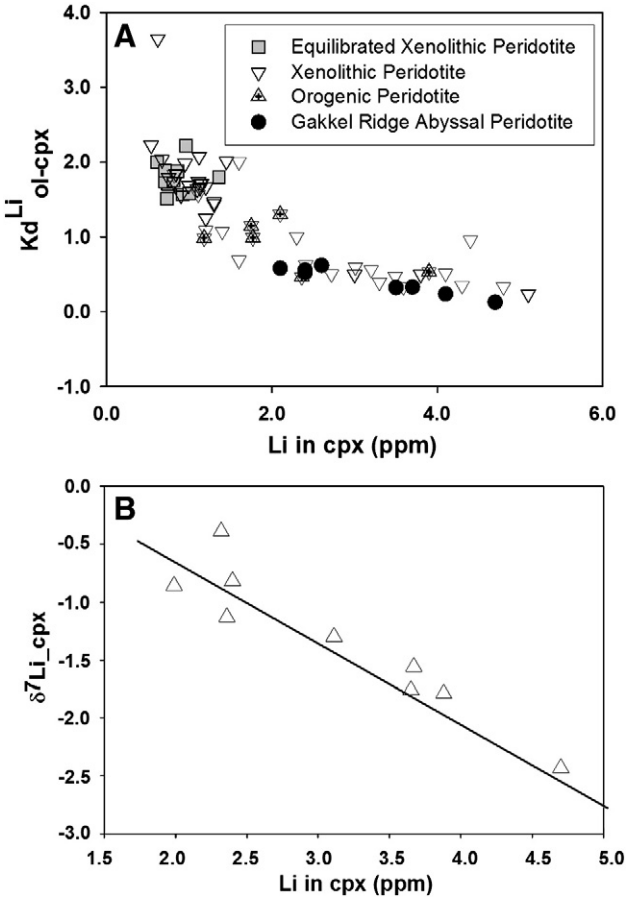

Fig. 1. Li elemental and isotopic compositions in clinopyroxene (cpx) and olivine (ol) separated from the fresh Gakkel Ridge abyssal peridotites. Also shown are mantle xenoliths from literature data (A), where Kd^{Li}_{ol-cpx} is defined as the ratio of C^{Li} (ppm) in olivine/C^{Li} (ppm) in cpx. The δ^7Li values of cpx are negatively correlated with their lithium concentrations (B).
Data sources are: Seitz and Woodland, 2000, for equilibrated xenolithic peridotites; Jeffcoate et al., 2007; Magna et al., 2006, 2008; Ottolini et al., 2004; Rudnick and Ionov, 2007; Seitz et al., 2004; Tang et al., 2007 for xenolithic peridotites; Ottolini et al., 2004, for orogenic peridotite.

0.06–0.16 ng Li. Compared with the ~150–200 ng Li used for our analysis, the blank correction is not significant at the uncertainty levels achieved.

Lithium isotopic compositions were analyzed at University of Maryland on a Nu Plasma MC-ICP-MS. We report results as $\delta^7Li = \{[(^7Li/^6Li)_{sample}/(^7Li/^6Li)_{standard}] - 1\}*1000$, relative to the L-SVEC Li-isotope standard. Details of the mass spectrometry are found in (Teng et al., 2004). The in-run precision on $^7Li/^6Li$ measurements is ≤0.2‰ for two blocks of 20 ratios each, with no systematic change in isotope ratio during each measurement session. The external precision, based on 2σ of repeated runs of international reference material for ultramafic rocks (DTS-2 and JP-1), is ≤1.0‰ (Gao and Casey, 2011, in press).

4. Results

Lithium abundances and isotopic compositions for mineral separate and bulk rock of Gakkel Ridge abyssal peridotite are reported in Table 1 and plotted in Figure 1.

Lithium concentrations vary on the order of clinopyroxene (2.1–4.7 ppm) > orthopyroxene (0.9–1.7 ppm) ≥ olivine (0.4–0.9 ppm) (Table 1), which is the opposite order of those found in equilibrated mantle peridotites (Ottolini et al., 2004; Seitz and Woodland, 2000). Compared with equilibrated peridotite xenoliths (Ottolini et al., 2004; Seitz and Woodland, 2000), Li is significantly enriched and depleted in coexisting clinopyroxene and olivine, respectively. This is illustrated in Figure 2A by the overall lower apparent Kd^{Li}_{ol-cpx} of 0.14 to 0.58 compared to that of ~1.7 for equilibrated peridotite (Ottolini et al., 2004; Seitz and Woodland, 2000).

The Li isotopic compositions indicate a systematic mineral variation (Table 1) with $\delta^7Li_{olivine}$ (7.14‰–15.09‰) > δ^7Li_{opx} (1.81‰–3.66‰) > δ^7Li_{cpx} (−2.43‰ to −0.39‰). δ^7Li values of orthopyroxene are mostly within its normal equilibrated mantle values of 1.8‰–4.0‰ (Ionov and Seitz, 2008). Olivines in pristine upper mantle have reported δ^7Li value of 3.6‰ to 3.8‰ (Magna et al., 2006). Thus, given the assumption of no significant inter-mineral isotopic fractionation at mantle temperature (Rudnick and Ionov, 2007), the studied olivine and clinopyroxene have significantly heavier and lighter δ^7Li values compared to those in the normal upper mantle, respectively. The δ^7Li values of clinopyroxene are negatively correlated with their Li concentrations (Fig. 1B). The observed Li isotopic fractionation between olivine and clinopyroxene ($\Delta^7Li_{olivine-cpx} = \delta^7Li_{olivine} - \delta^7Li_{cpx}$) is in general negatively correlated with the apparent Li partition coefficient ($Kd^{Li}_{ol-cpx} = [Li]_{ol}/[Li]_{cpx}$).

In contrast to the variable and fractionated isotopic compositions in olivine and cpx, the studied Gakkel Ridge peridotites have δ^7Li values ranging from 3.03‰ to 4.53‰ with an average of 3.7 ± 0.6‰, which is close to the reported δ^7Li value of ~+3.5‰ for the pristine

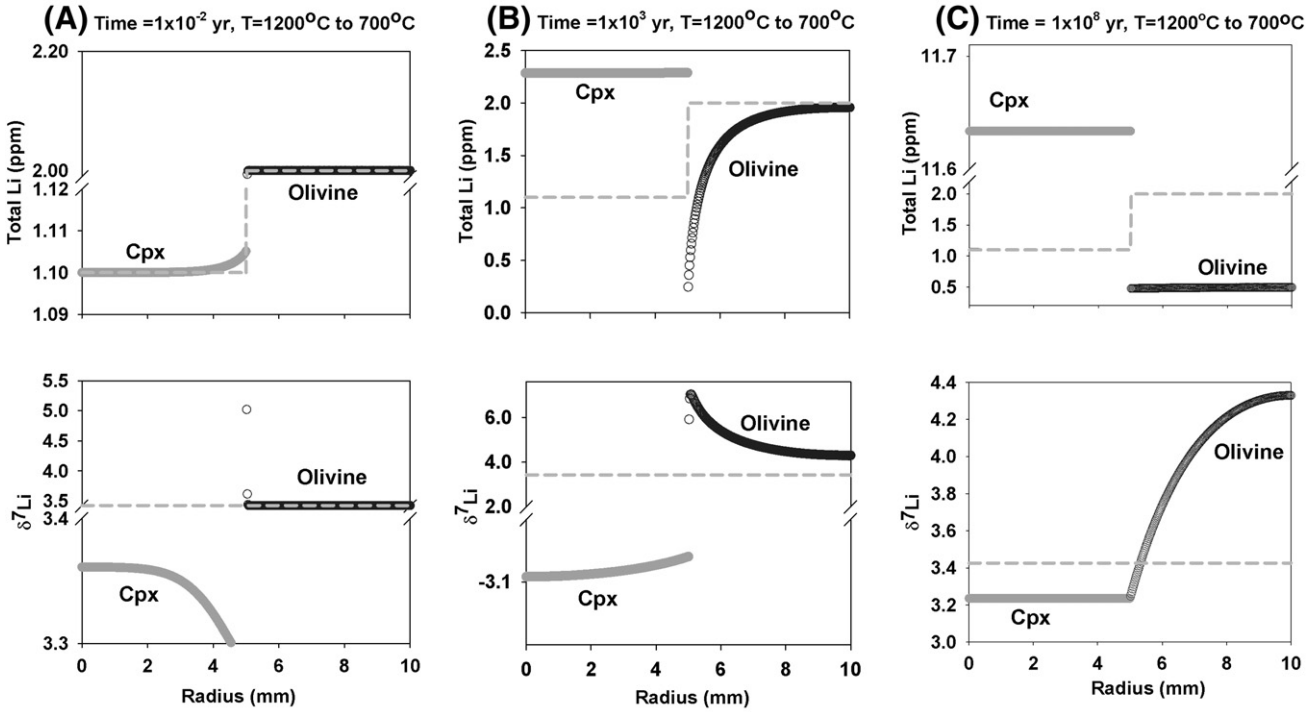

Fig. 2. Numerical modeling results of total Li concentration and Li isotopic composition (δ^7Li) variation in a closed system using a Robin boundary condition and temperature dependent diffusivity and partition coefficient, as described in the text. Light color filled circle represents clinopyroxene, dark color open circle represents olivine, and grey dashed line represents initial values of Li and δ^7Li. The radius of olivine and the enclosed clinopyroxene is 10 mm and 5 mm, respectively (assuming assuming cpx and olivine are concentric). The cooling rates are defined to cool the mantle rock from 1200 °C to 700 °C at time duration of 1×10^{-2} years (A), 1×10^{3} years (B) and 1×10^{7} years (C).

upper mantle (Jeffcoate et al., 2007; Magna et al., 2006). Li concentration and isotopic compositions in bulk rock were also calculated using the modal analysis in Table 1.

Except for sample PS66-238-18, the reconstructed bulk rock compositions are systematically lower in concentration and heavier in isotopic composition than the measured values (Table 1). Sample PS66-238-18 has the closest values for both Li content (1.54 ppm vs. 1.66 ppm) and isotopic composition (3.14‰ vs. 3.27‰) between calculated and analyzed compositions. The apparent deviation between analyzed and reconstructed bulk rock values could suggest the presence of inter-grain phases. However, the calculated Li concentrations are in fact generally *lower* than the measured values, which eliminates the possible presence of unaccounted Li bearing phases beside the major component minerals. The absence of any other inter-grain phases was also supported by the detailed thin section observations. Calculations using different modal compositions showed that the reconstructed bulk rock values could not be significantly changed by increasing the modal proportions of cpx up to 10% (hence a decrease of 10% for olivine). Thus, the difference is considered to reflect the likelihood that not all olivine grains experienced inter-mineral redistribution during cooling. Those olivine grains far away from any clinopyroxene grains should have retained their original upper mantle values of higher Li content and lower δ^7Li compositions compared to the fractionated grains (see details in the following sections). This could also be a sampling bias during the mineral separation, such as the preferential loss of the rims for clinopyroxenes (as they were in close contact with other minerals), which tend to have high Li contents and light δ^7Li values. The likelihood of losing the outer portions of mineral separate during the preparation process was also proposed by Jeffcoate et al. (2007).

5. Discussion

As illustrated in Figures 2 and 3, the observed inter-mineral fractionations appears to be the result of a redistribution of Li between minerals as a result of sub-solidus cooling driven by temperature, or less likely to pressure dependent inter-mineral partitioning. During cooling, Li becomes less compatible in olivine compared with clinopyroxene. A diffusive redistribution of Li during cooling then results in mass-dependent Li isotopic fractionation. Alternatively, Li exchange via melt–rock reaction may have occurred. Melt refertilization is common in abyssal peridotites from slow-spreading ridges (Seyler et al., 2004). However, the pristine normal upper mantle values for Li and its isotopic composition of the bulk rocks suggest that the studied peridotites may not have undergone significant melt refertilization or the melt–rock interaction did not modify the Li isotopic system significantly. Inter-mineral diffusive exchange, rather than modification by an external melt, is also indicated by the observed simultaneous anti-correlation of Li content in olivine and the coexisting clinopyroxene (Fig. 1).

5.1. Numerical modeling

In order to test whether diffusion-driven fractionation by cooling alone is sufficient to produce the observed Li elemental and isotopic fractionation, we have conducted numerical diffusion modeling. Given the assumptions we make, the modeling result will provide a theoretical basis for understanding both our data and for interpreting Li-isotope variations in mantle and volcanic rocks in general. Such information is crucial to explore how the Li-isotope system can potentially constrain the cooling history and the mechanism of emplacement of the upper oceanic mantle beneath mid-ocean ridges.

This model considers the diffusion of Li from a host mineral (spherical olivine) into an enclosed mineral (spherical clinopyroxene). This is set to mimic the natural occurrence of clinopyroxene in most peridotites. The partition coefficients of Li between olivine and clinopyroxene decrease during cooling, so that the concentration gradient will drive a diffusive redistribution of Li. The transport of Li in both olivine and clinopyroxene is controlled by a temperature dependent radial diffusion.

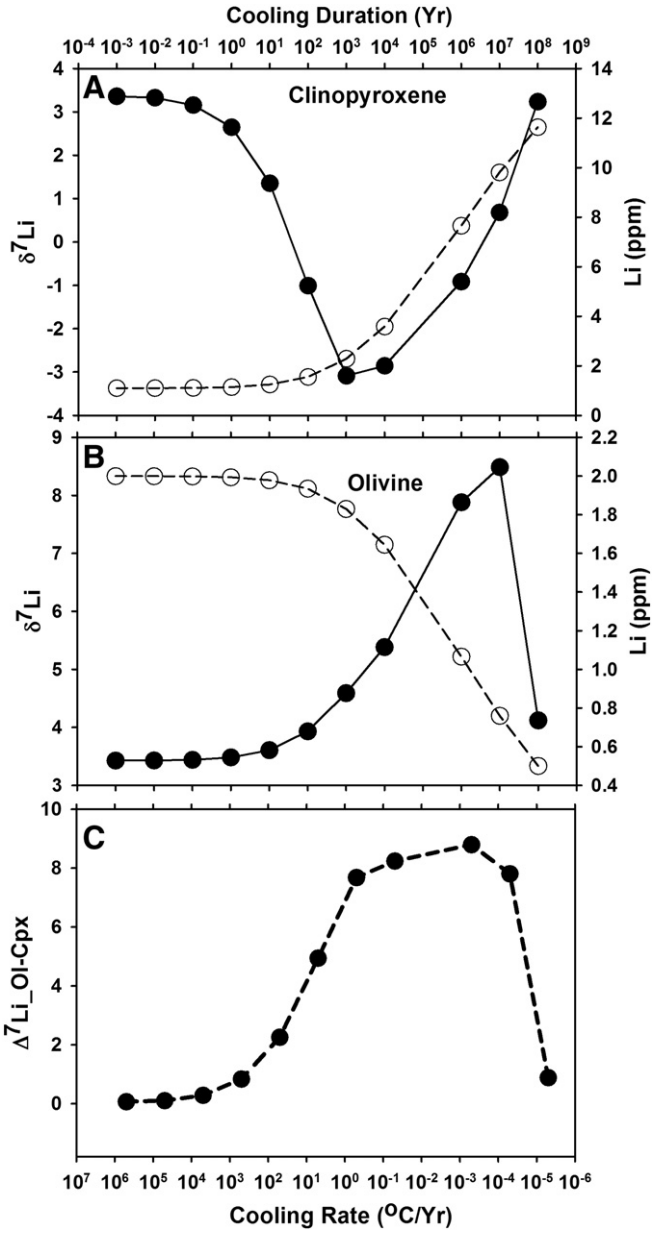

Fig. 3. Predicted variation of average Li concentration (open circle), average Li isotopic composition (filled circle) in clinopyroxene (A) and olivine (B) and isotopic fractionation between olivine and clinopyroxene (C) at given cooling durations as a result of cooling induced diffusive exchange of Li. The cooling rates are defined to cool the mantle rock from 1200 °C to 700 °C at given duration. Modeling parameters are same as those for Figure 2. With the progressive increase of cooling duration, Li migrated gradually from olivine into clinopyroxene and given long enough time the average concentration of Li in olivine and clinopyroxene eventually fixed at concentrations defined by the Kd^{Li}_{ol-cpx} at 700 °C. As ^{6}Li travels faster than ^{7}Li, in shorter diffusion duration, the net incoming flux of Li into clinopyroxene is dominated by ^{6}Li, leading to a decrease of δ^7Li value in clinopyroxene and a counter balanced increase of δ^7Li value in olivine. With the increase of diffusion duration, at one point, the net flux of Li became dominated by ^{7}Li and thus the clinopyroxene returned to be heavier and olivine to be lighter from their low and high peak, respectively.

The general equation for diffusion in a sphere is (Crank, 1975):

$$\frac{\partial C}{\partial t} = D(T)\left(\frac{\partial^2 C}{\partial r^2} + \frac{2}{r}\frac{\partial C}{\partial r}\right) \quad (1)$$

where C refers to the concentration at position r after time t, r is distance to the sphere center ($r=0$), and D(T) is the temperature dependent diffusion coefficients. The boundary and initial conditions are taken as following, where a is the radius of clinopyroxene and A is the radius of olivine (assuming cpx and olivine are concentric):

$$\frac{\partial C}{\partial r} = 0, r = 0, r = A, t > 0 \quad (2)$$

$$D^{\text{Olivine}}(T)\frac{\partial C}{\partial r} = D^{\text{cpx}}(T)\frac{\partial C}{\partial r}, r = a, t > 0 \quad (3)$$

$$C_{\text{olivine}} = Kd^{Li}_{ol-cpx}(T)C_{\text{cpx}}, \quad \text{r} = \text{a}, \text{t} \geq 0 \quad (4)$$

$$C_{\text{cpx}} = 1.1, C_{\text{olivine}} = 2.0, \quad t = 0, 0 \leq r \leq \text{A} \quad (5)$$

The bulk concentration of ^{7}Li or ^{6}Li in cpx and olivine at any given time is given by the integrals:

$$C^{n_{Li}}_{cpx} = \int_0^a 4\pi r^2 C^{n_{\text{Li}}}_{\text{cpx}} dr \quad (6)$$

$$C^{n_{Li}}_{olivine} = \int_a^A 4\pi r^2 C^{n_{\text{Li}}}_{\text{olivine}} dr \quad (7)$$

where $C^{n_{Li}}$ is the concentration of the respective Li isotope at given point within the mineral grain. The bulk Li concentration and bulk isotope composition is defined by the sum of ^{7}Li and ^{6}Li and the ratio of ^{7}Li/^{6}Li, respectively.

Boundary conditions described by Eqs. (2)–(4) are based on the assumptions: (1) Li content and its isotopic composition are initially equilibrated at mantle temperature and uniformly distributed in olivine and the enclosed clinopyroxene; (2) conservation of flux across the boundary between olivine and clinopyroxene are maintained during diffusion and (3) chemical equilibrium of Li between olivine and clinopyroxene is maintained at all times at the contact boundary ($r=$a), and (4) there is no diffusion at the sphere center ($r=0$) and the surface of the sphere ($r=$A) at any time.

The initial concentrations of Li in olivine and clinopyroxene are set to be 1.1 ppm and 2.0 ppm, respectively. This is derived from the available mineral data of equilibrated peridotites from mantle xenoliths (Ionov and Seitz, 2008; Ottolini et al., 2004; Seitz and Woodland, 2000). The initial δ^7Li values for olivine and clinopyroxene are set to be $\delta^7\text{Li}_{\text{ol}} = \delta^7\text{Li}_{\text{cpx}} = 3.5‰$, based on the analysis of pristine olivine (unaltered) in upper mantle (Jeffcoate et al., 2007; Magna et al., 2006, 2008; Seitz et al., 2004) and the assumption of zero Li isotopic fractionation at mantle temperature (Rudnick and Ionov, 2007).

Equilibrium Li isotopic fractionation at mantle temperatures is not well constrained, as no experimental data are yet available. Fractionation coefficients are currently estimated from empirical studies (Jeffcoate et al., 2007; Rudnick and Ionov, 2007 and references therein). In contrast to the wide range of possible values for $\Delta^7\text{Li}_{\text{ol-cpx}}$ from −5 to 4 (Jeffcoate et al., 2007; Seitz et al., 2004), Rudnick and Ionov (2007) proposed that the equilibrium $\Delta^7\text{Li}_{\text{ol-cpx}}$ at mantle temperature is zero. This debate is largely derived from the fact that the Li isotopic compositions of the constituent minerals in the mantle (especially clinopyroxene) could be fractionated by diffusive transportation of ^{7}Li and ^{6}Li in the process of metasomatism by fluid or melt (Jeffcoate et al., 2007; Lundstrom et al., 2005; Magna et al., 2008; Rudnick and Ionov, 2007; Teng et al., 2006). For this modeling, we initially set the $\Delta^7\text{Li}_{\text{ol-cpx}}$ to be constant of zero (i.e. no fractionation) during cooling, the possible effect of a temperature dependent $\Delta^7\text{Li}_{\text{ol-cpx}}$ was evaluated later by simulation.

The temperature dependent diffusivity of ^{6}Li in clinopyroxene was experimentally determined by Coogan et al. (2005) as: $D^{6_{Li}}(T) = D_0 e^{-\frac{E}{RT}}$, where $D_0 = 0.029\ \text{m}^2\ \text{s}^{-1}$ and $E = 258\ \text{kJ mol}^{-1}$. A slower diffusion rate has also been speculated by theoretical modeling of the zoning profiles in natural clinopyroxenes (Jeffcoate et al., 2007; Parkinson et al., 2007), though no temperature dependent diffusivity

of Li could be derived from such studies. The diffusivity of Li in mantle olivine is still poorly constrained and seems to be a very complex process depending not only on chemical environment but also on diffusion mechanisms in addition to temperature and pressure (Dohmen et al., 2010). The experimental study (Dohmen et al., 2010) showed that the Li diffusion rate in most natural olivines could be approximately described by $\log(D_{Li}) = -5.92(\pm 1.0) - 1.2847\times 10^4/T(K)$. This experimentally determined Li diffusion rate in olivine is significantly slower than that in clinopyroxene, though it is about 10 times faster than that previously estimated by the theoretical modeling (Parkinson et al., 2007). The low diffusion rate of Li in olivine has been speculated as a result of coupled exchange of Li with P, which is one of the slowest diffusing elements in olivine (Mallmann et al., 2009). For this modeling purpose, the experimentally derived diffusion data given by Coogan et al. (2005) for clinopyroxene and Dohmen et al. (2010) for olivine were used for calculations in the first place. The possible effect of variable diffusion rates on the modeling results will be discussed later. The diffusivity of ^{7}Li is given by $\frac{D_7}{D_6} = \left(\frac{m_6}{m_7}\right)^{0.215}$ (Parkinson et al., 2007; Richter et al., 2003), indicating a faster (~3.35%) diffusion of ^{6}Li than ^{7}Li. The variation of Li partition coefficient between olivine and clinopyroxene with temperature is speculated from the experimentally determined partitioning data of Li between clinopyroxene and plagioclase. Coogan et al. (2005) reported a linear relationship between 1000/T and ln(kd) for the Li partitioning between plagioclase and cpx, where Li becomes more compatible into clinopyroxene at lower temperatures. For simplicity of the modeling, a similar linear correlation was assumed for olivine and clinopyroxene pair as

$$ln(Kd^{Li}_{ol-cpx}) = -10900/T + 8.0 \quad (8)$$

The slope and intercept of the linear equation were set to give a best fit of the reported Kd^{Li}_{ol-cpx} values at mantle temperature (Eggins et al., 1998; Ottolini et al., 2004; Seitz and Woodland, 2000). The assumed linear correlation leads to Kd^{Li}_{ol-cpx} to be 1.82 at 1200 °C and 0.04 at 700 °C.

Given these constraints, the set of equations presented are solved numerically using a finite element method programmed with Matlab®. Compared to existing models of Li diffusion in a single grain (Gallagher and Elliott, 2009; Parkinson et al., 2007), this model represents a closed system, which includes an internal Robin boundary condition together with temperature dependent diffusivity of Li in both olivine and cpx and temperature dependent partition coefficients between olivine and cpx.

5.1.1. Model results

Modeling results of clinopyroxene enclosed by olivine under different cooling rate are shown in Figure 3. The cooling rates correspond to the duration over which the mantle was cooled down from 1200 °C to 700 °C. The effective diffusive exchange of Li between clinopyroxene and olivine will eventually cease when it has been cooled down to the closure temperature of one of the two minerals. The closure temperature depends on the diffusion parameters, the cooling rate and the grain size. The mean closure temperature was calculated by the equation given by Dodson (1973) as:

$$T_c = \frac{E/R}{ln\left[-\frac{ART_c^2(D_0/a^2)}{EdT/dt}\right]} \quad (9)$$

where E is the activation energy for diffusion of Li in clinopyroxene; A is 55; R is the gas constant; D_0 is the pre-exponential factor in Arrhenius relation; a is the grain radius and dT/dt is the cooling rate, and Tc is the closure temperature in Kelvin.

The estimated cooling rates in studied mantle rocks are about 30 °C/Ma to 130 °C/Ma (Von de Handt, 2008). The diffusion of Li in olivine has been reported to be about 3 orders of magnitude slower than that in clinopyroxene (Coogan et al., 2005; Dohmen et al., 2010). Thus the effective closure temperature Li in the studied two-mineral system will be actually given by that in olivine which is higher than that in clinopyroxene. The calculations show that the closure temperatures in a spherical olivine grain of 10 mm radius vary from 690 °C to 730 °C, depending on the cooling rate. For simplicity, thus, the cessation temperature of the modeling is set to be 700 °C. Similar to other reported models (Beck et al., 2006; Gallagher and Elliott, 2009; Parkinson et al., 2007), our results illustrate that a diffusion process in a closed system alone is sufficient to produce significant Li elemental and isotopic change within minerals. Due to the decrease of compatibility of Li in olivine during cooling, Li progressively migrates out of olivine into clinopyroxene. As ^{6}Li diffuses faster than ^{7}Li, the enrichment and depletion of Li in clinopyroxene and olivine produce fractional δ^7Li profiles.

Both the shape of zoning profile and fractionation factor between olivine and clinopyroxene are sensitive to cooling rate (Fig. 2). Li progressively moves out from olivine and enters into clinopyroxene, which is due to the decrease of Kd^{Li}_{ol-cpx} during cooling. Zoning profiles of δ^7Li in clinopyroxene with heavier values at core and lighter values towards rim (reversed bowl shape) are preserved for fast cooling events, reflecting the faster diffusion of ^{6}Li than ^{7}Li (Fig. 2A). The reversed bowl shaped zoning profile of δ^7Li in clinopyroxene was accompanied by a normal bowl shaped zoning in olivine with heavier δ^7Li at rim. The predicted reversed bowl shaped zoning profiles for δ^7Li have been reported in clinopyroxene phenocrysts in Hawaiian basalts (Jeffcoate et al., 2007) and in Solomon Islands arc lavas (Parkinson et al., 2007), which formed under rapid/instantaneous cooling. For slower cooling rates, normal bowl shaped profiles in clinopyroxene with gradually increased δ^7Li values toward the rim are predicted by the modelling (Fig. 2B). The changing of zoning patterns of δ^7Li in clinopyroxene reflects the increased incoming flux of ^{7}Li from olivine to maintain the mass balance of total Li in a closed system. Owing to the fact that ^{6}Li travels faster than ^{7}Li, with shorter diffusion duration, the net incoming flux of Li into clinopyroxene is dominated by ^{6}Li, leading to a decrease of δ^7Li value in clinopyroxene and a counter balanced increase of δ^7Li value in olivine (Figs. 2 and 3A, B). However, when the cooling rate decreases further, at one point, the net flux of Li from olivine into clinopyroxene will be dominated by ^{7}Li and thus leads to clinopyroxene and olivine to become heavier and lighter in δ^7Li values, respectively (Figs. 2C and 3A, B). The exact position of this turning around point depends on the relative grain size, relative diffusivity, and the temperature dependence of Kd^{Li}_{ol-cpx} and $\Delta^7Li_{\_Ol-Cpx}$. Under the given parameters in the modelling, the change of the dominant species of Li isotope occurred at cooling rate of ~1 °C/year (Fig. 3). The change in the dominant isotope species (i.e. ^{6}Li or ^{7}Li) of cooling induced diffusive net Li flux between olivine and clinopyroxene is a consequence of maintenance of the isotopic equilibration. There is always a tendency for the Li system to return to its equilibrium status given enough time, which is also the driving force for diffusion. As shown in Figure 3C, the predicted inter-mineral fractionation, $\Delta^7Li_{\_Ol-Cpx}$, first increased along with the increase of cooling duration and then decreased toward its equilibrium status ($\Delta^7Li_{\_Ol-Cpx} = 0$ at all time) after reaching its highest value. The effect of a temperature dependent $\Delta^7Li_{\_Ol-Cpx}$ on the modelling is discussed latter. The simulation results illustrate that the bulk compositions of Li and δ^7Li in clinopyroxene and olivine are dominantly determined by its cooling history (Fig. 3).

Most strikingly, these simple models show that the negative δ^7Li values for clinopyroxene due to the diffusive exchange of Li with olivine can only be preserved at a certain range of cooling rates (Figs. 2 and 3A, B). The Li isotopic fractionation between olivine and clinopyroxene is predicted to be strongly dependent on cooling rate and can change its fractionation direction with a decreased cooling rate (Fig. 3C).

Though Li zoning profiles in both mineral phases are predicted by the modelling results, the core to rim variations of Li content and δ^7Li values in clinopyroxene are quite small compared to that in olivines (Fig. 2). The small core to rim variation of Li systematic in clinopyroxenes could be explained by its much faster diffusion rate (~4 orders of magnitude) of Li compared to that in olivines. So in practice, zoning patterns of Li in clinopyroxenes will be hardly detected given the currently analytical precisions. Efforts to study Li zonings in mantle minerals should be mainly focused on olivines.

5.1.2. Influence of input parameters

Physically, besides cooling rate, the predicted diffusion profiles will also depend on other input parameters, such as the relative grain sizes of olivine and clinopyroxene, the temperature dependence of diffusivity of Li in olivine and clinopyroxene, and the temperature dependence of Li partitioning between olivine and clinopyroxene.

5.1.2.1. Relative grain size. To evaluate the effect of relative grain size between olivine and its enclosed clinopyroxene, we ran a series of simulations using the same initial and boundary conditions given in the previous modelling, but set the radii of the crystals to be 1 mm for clinopyroxene and 10 mm for olivine. The simulation results illustrated that the general dependence between diffusion profile and cooling rate/cooling duration remains the same as those with small radius ratio shown in Figure 2. However, the large radius ratio of olivine to clinopyroxene (10 to 1) could generate a larger variation of Li content and Li-isotope composition in clinopyroxene and a smaller variation in olivine (Fig. 4). This is expected considering the mass balance effect between olivine and clinopyroxene. The smaller grain size of clinopyroxene compared to its host mineral, olivine, makes its composition more sensitive to a diffusion exchange of Li during cooling. Hence, smaller grains of clinopyroxene may appear to have more depleted δ^7Li composition but an enriched Li content in mantle rocks that have experienced a cooling process in a closed system.

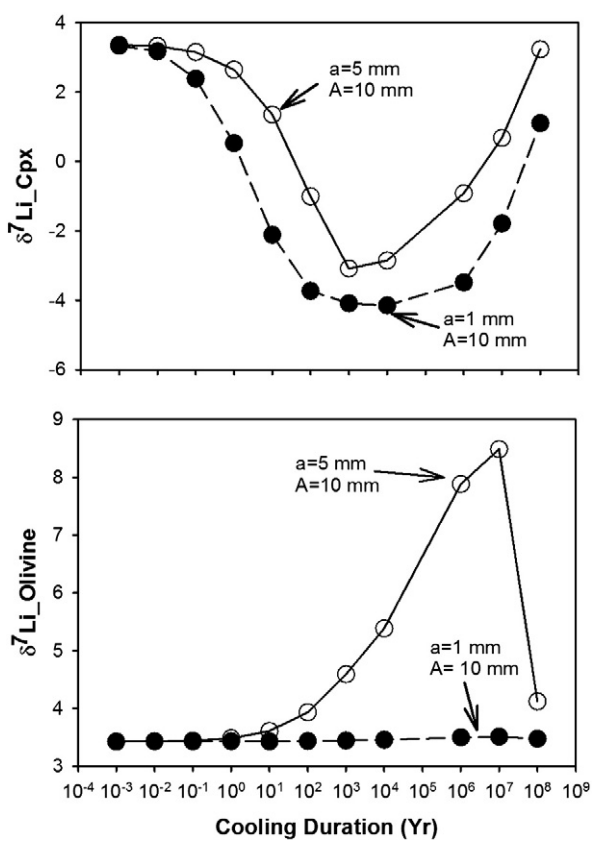

Fig. 4. Predicted Li isotopic variations in olivine and its enclosed clinopyroxene at different grain size ratios, where *a* and A is the radius for clinopyroxene and olivine, respectively. Except for grain size, other parameters are same as those given in Figure 2.

5.1.2.2. Relative diffusivity. In modelling mentioned, the adapted Li diffusivities given by Coogan et al. (2005) and Dohmen et al. (2010) result to the diffusion rate of Li in olivine to be about 3–4 orders of magnitude slower than that in clinopyroxene at the temperature range from 700 °C to 1200 °C. It has been found that Li could also diffuse at a much faster rate via interstitial mechanism in olivine, though it is unlikely to be the dominant mechanism in most natural systems (Dohmen et al., 2010). We ran simulations to examine the effect of diffusivity on diffusive exchange by assuming a same diffusivity of Li in olivine as that in clinopyroxene.

As expected, a faster diffusion rate in olivine leads to a more rapid response of the Li system to the cooling driven diffusive exchange. The Li concentration in clinopyroxene in contact with an olivine with a fast Li diffusion rate increases more rapidly compared to that with slow diffusion rate in olivine, and thus lead to a higher Li concentration in clinopyroxene at given cooling duration (Fig. 5A). At given cooling rate, faster Li diffusion in olivine causes more depleted and more enriched δ^7Li values in clinopyroxene before and after reaching the turning around point for dominant isotope type of Li flux (Fig. 5B). The modelling results showed that a slower Li diffusion in olivine could result the depleted δ^7Li values in clinopyroxene to be preserved for a much longer time, though the minimum δ^7Li in clinopyroxene is predicted to be a bit higher than that with a faster Li diffusion in olivines (Fig. 5B). The final compositions of Li and its isotope in clinopyroxene at given temperature (i.e. 700 °C in this case) are defined by the cooling duration/cooling rate and will eventually reach equilibrium state for a long cooling duration (Fig. 5).

5.1.2.3. Temperature dependence of Kd^{Li}_{ol-cpx}. To examine the role of Kd^{Li}_{ol-cpx} in the modeling, we rescaled the temperature dependence of Kd^{Li}_{ol-cpx} given in Eq. (8) to be:

$$ln(Kd^{Li}_{ol-cpx}) = -2061 / T + 2.0 \quad (10)$$

Eq. (10) gives a small decrease of the partition coefficients from 1.82 to 0.89 during cooling from 1200 °C to 700 °C. The simulation results are shown in Figure 6. As expected, the lower degree of temperature dependence of Kd^{Li}_{ol-cpx} yielded a smaller fractionation of δ^7Li in clinopyroxene during cooling (Fig. 6A). The degree of inter-mineral isotopic fractionation is also decreased (Fig. 6B). This is a logical result, as the temperature dependent variation of Kd^{Li}_{ol-cpx} is the ultimate driving force of the diffusive redistribution of Li between olivine and clinopyroxene.

5.1.2.4. Temperature dependence of $\Delta^7Li_{\_Ol-Cpx}$. There are, so far, no existing data on the temperature dependence of equilibrium fractionation between olivine and clinopyroxene, though a temperature dependent fractionation between clinopyroxene and fluids has been reported (Wunder et al., 2006). The temperature dependence of Δ^7Li$_{_Ol-Cpx}$ was simulated by giving different Kd^{Li}_{ol-cpx} to ^{7}Li and ^{6}Li at different temperature. We assumed that Kd_{ol-cpx} ^{6}Li decreases more rapidly than Kd_{ol-cpx} ^{7}Li along cooling, thus Δ^7Li$_{_Ol-Cpx}$ increases with the decrease of temperature. For similarity, we arbitrarily assume the temperature dependence of Kd_{ol-cpx} ^{6}Li follows Eq. (8) and Kd_{ol-cpx} ^{7}Li follows the Eq. (11), respectively, which leads to the Δ^7Li$_{_Ol-Cpx}$ increases from ~0 to ~22 when the system cooled down from 1200 °C to 700 °C.

$$ln(Kd^{Li}_{ol-cpx}) = -10826 / T + 7.95 \quad (11)$$

Compared to the constant Δ^7Li$_{_Ol-Cpx}$ = 0 during cooling, the assumption of an increased Δ^7Li$_{_Ol-Cpx}$ with the decrease of

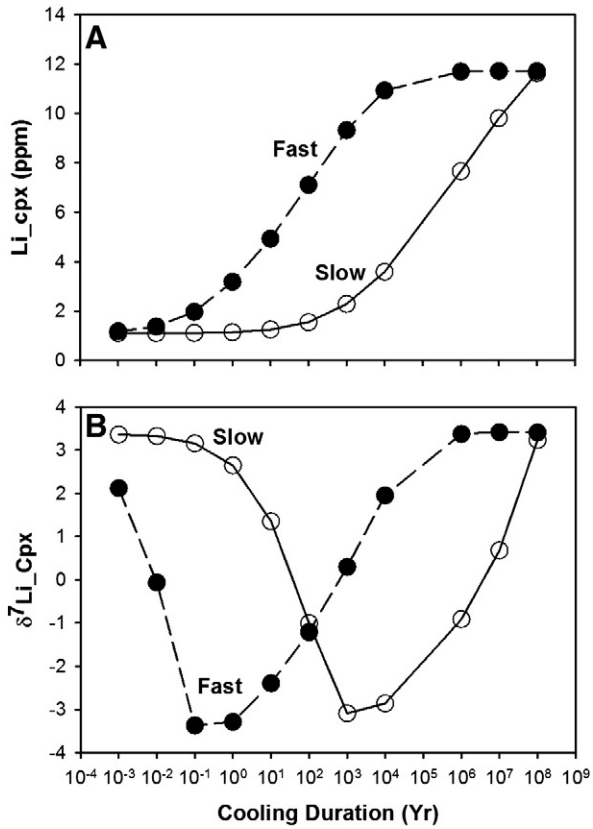

Fig. 5. Predicted Li elemental and isotopic variations in olivine and its enclosed clinopyroxene for different diffusion rate of Li in olivine, where open circle and filled circle represent slow and fast diffusion rate, respectively (see text for details). Except for Li diffusion rate in olivine, other parameters are same as those given in Figure 2.

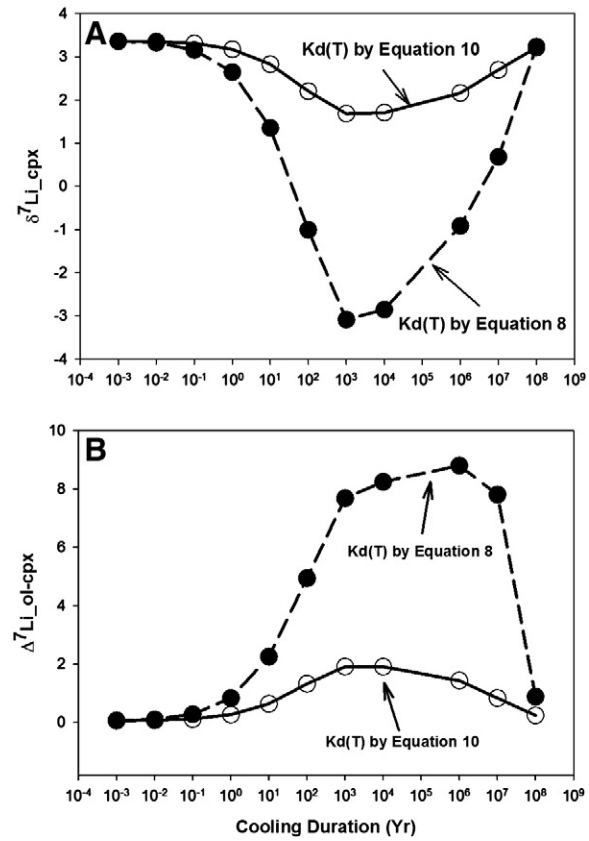

Fig. 6. Predicted average Li isotopic composition (A) and inter-mineral isotopic fractionation (B) in olivine and its enclosed clinopyroxene for different temperature dependence of Kd^{Li}_{ol-cpx}, where filled circle and open circles represent Kd (T) defined by Eqs. (8) and (10), respectively (see text for details). Except for Kd^{Li}_{ol-cpx}, other parameters are same as those given in Figure 2.

temperature could yield a much larger isotopic fractionation at given cooling rate/cooling duration (Fig. 7A). The temperature dependent $\Delta^7Li_{\_Ol-Cpx}$ also yields a much lighter δ^7Li in clinopyroxene (Fig. 7B). Compared with the constant $\Delta^7Li_{\_Ol-Cpx}$ during cooling, the negative δ^7Li values in clinopyroxene could survive a much longer cooling duration of up to million years under the assumed conditions (Fig. 7B).

5.2. Cooling driven diffusive Li elemental and isotopic fractionation

The systematic inter-mineral fractionations together with the pristine normal upper mantle values of the bulk rocks suggested the fresh abyssal peridotites exposed at Gakkel Ridges may have experienced a redistribution of Li between minerals in a closed system as a result of sub-solidus cooling driven by temperature. The numerical simulations illustrated that the process of cooling alone is sufficient to generate significant Li elemental and isotopic fractionation. Such a conclusion has been suggested by the general consistency between numerical modeling and the observations of Li systems in phenocrysts enclosed by rapid cooled lavas (Gallagher and Elliott, 2009). It has also been speculated based on a statistical comparison study of mantle xenoliths recovered from different tectonic and magmatic environments (Ionov and Seitz, 2008).

However, due to the rapid diffusion rate of Li at high temperatures, the fractionated isotopic signatures could be smoothed out in very short time duration. This has limited the usage of Li as a geospeedometer to those processes that occurred over only a few hours to few hundreds of days (Coogan et al., 2005; Gallagher and Elliott, 2009; Ionov and Seitz, 2008; Parkinson et al., 2007). Our new modeling results (Fig. 7) showed that inter-mineral isotopic disequilibrium in the Li system could potentially survive for millions of years, assuming the exchange of Li has only occurred between two-mineral phases in a closed system. The key factor to preserve the disequilibrium is the presence of a temperature dependent inter-mineral partition coefficients and continuous cooling till the closure temperature (i.e. no significant long pause at any temperature higher than the closure temperature). As illustrated by the modeling, a temperature dependent Li isotopic fractionation between olivine and clinopyroxene ($\Delta^7Li_{\_Ol-Cpx} = f(T)$) could result to the preservation of negative Li isotopic compositions ($\delta^7Li<0$) in clinopyroxene for millions of years (Fig.7).

Based on the full spreading rate of 13.2 mm/year (Jokat et al., 2003) and the assumption that only passive upwelling is present at the sample location (e.g. Shen and Forsyth, 1995), an uplift rate of about 6.6 km/Ma has been expected for the studied peridotites (Von de Handt, 2008) . The depth to 1200 °C isotherm beneath the ridge-axis was estimated to be about 25–30 km extrapolating from the modeling results given by Phipps Morgan and Chen (1993). Given these constraints, the cooling durations of the studied mantle samples were estimated to be 3–5 million years. Despite of this long cooling duration, negative δ^7Li compositions in clinopyroxenes along with large isotopic fractionations with olivines were preserved in the studied peridotites (Table 1). According to the modelling results (Fig. 7), this observation would suggest that the $\Delta^7Li_{\_Ol-Cpx}$ to be temperature dependent. However, the studied mantle rocks may have been cooled with variable cooling rates, such as a late stage rapid cooling following an initial slow cooling. Though a variable cooling rate is less likely given the tectonic setting, the definite answer to this question will depend on experimental determination of the temperature dependence of Kd^{Li}_{ol-cpx} and $\Delta^7Li_{\_Ol-Cpx}$.

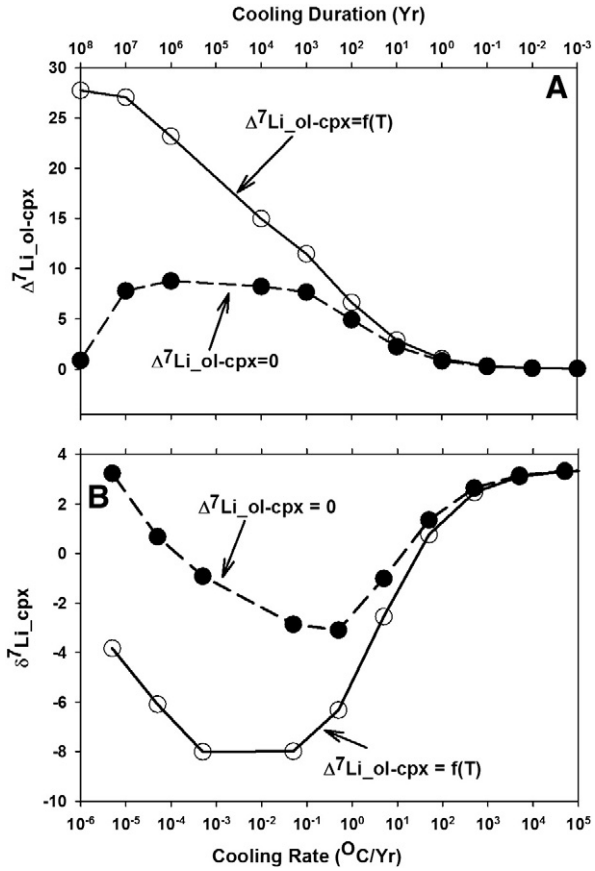

Fig. 7. Predicted inter-mineral isotopic fractionation (A) and average Li isotopic composition (B) in olivine and its enclosed clinopyroxene for different temperature dependence of $\Delta^7Li_{\_Ol-Cpx}$, where open circle and filled circles represent $\Delta^7Li_{\_Ol-Cpx} = f(T)$ and $\Delta^7Li_{\_Ol-Cpx} = 0$, respectively. The modeled mantle rock was assumed to be cooled continuously from 1200 °C to 700 °C at given time duration. Except for $\Delta^7Li_{\_Ol-Cpx}$, other parameters are same as those given in Figure 2.

6. Conclusions

(1) The observed systematic inter-mineral variations of Li concentrations and isotopic compositions could be explained by a cooling driven diffusive redistribution between minerals in a closed system.

(2) The preservation of extremely light δ^7Li clinopyroxenes (significantly lighter than its normal mantle value of ~3.5‰) and the large $\Delta^7Li_{\_Ol-Cpx}$ suggest that the Li elemental and isotopic equilibrium fractionation between olivine and clinopyroxene is temperature dependent. The studied Gakkel Ridge abyssal peridotites may alternatively have cooled under a variable cooling rate with a rapid cooling before the Li system was closed, which is less likely given the tectonic setting.

(3) Li systematics in minerals, especially in coexisting mineral phases can be potentially used as a geospeedometer even for slowly cooled rocks. However, this application will be largely depend on the accurate knowledge on the temperature dependence of Kd^{Li}_{ol-cpx} and $\Delta^7Li_{\_Ol-Cpx}$.

(4) Cautions should be taken to interpret the disequilibrium in Li isotopic data in mantle minerals as indicators for material recycling and/or metasomatism in mantle.

Acknowledgements

We thank W. McDonough and R. Rudnick for their kind support for Li-isotope analysis and discussions on the preliminary results. The manuscript benefited from careful reviews by T. Magna and one anonymous reviewer, as well as from the editorial work by R. Carlson. We thank the crew and onboard scientists on the ARK-XX expedition to Gakkel Ridge, and the Alfred-Wegener Institute for Marine and Polar Research, Bremerhaven, Germany. J. F. Casey acknowledges the support by NSF OCE-0351646. The CAS/SAFEA International Partnership Program for Creative Research Teams partially provided financial support for this study.

References

Beck, P., Chaussidon, M., Barrat, J.A., Gillet, P., Bohn, M., 2006. Diffusion induced Li isotopic fractionation during the cooling of magmatic rocks: the case of pyroxene phenocrysts from nakhlite meteorites. Geochim. Cosmochim. Acta 70, 4813–4825.

Berger, G., Schott, J., Loubet, M., 1987. Foundamental processes controlling the first stage of lateration of a basalt glass by seawater: an experimental study between 200 and 320 °C. Earth Planet. Sci. Lett. 84, 431–445.

Berger, G., Schott, J., Guy, C., 1988. Behavior of Li, Rb and Cs during basalt glass and olivine dissolution and chlorite, smectite and zeolite precipitation from seawater: experimental investigations and modelization between 50 °C and 300 °C. Chem. Geol. 71, 297–312.

Bouman, C., Elliott, T., Vroon, P.Z., 2004. Lithium inputs to subduction zones. Chem. Geol. 212, 59–79.

Brenan, J.M., Neroda, E., Lundstrom, C.C., Shaw, H.F., Ryerson, F.J., Phinney, D.L., 1998a. Behaviour of boron, beryllium, and lithium during melting and crystallization: constraints from mineral-melt partitioning experiments. Geochim. Cosmochim. Acta 62, 2129–2141.

Brenan, J.M., Ryerson, F.J., Shaw, H.F., 1998b. The role of aqueous fluids in the slab-to-mantle transfer of boron, beryllium, and lithium during subduction: experiments and models. Geochim. Cosmochim. Acta 62, 3337–3347.

Brooker, R.A., James, R.H., Blundy, J.D., 2004. Trace elements and Li isotope systematics in Zabargad peridotites: evidence of ancient subduction processes in the Red Sea mantle. Chem. Geol. 212, 179–204.

Chan, L.H., Edmond, J.M., 1988. Variation of lithium isotope composition in the marine-environment — a preliminary-report. Geochim. Cosmochim. Acta 52, 1711–1717.

Chan, L.H., Edmond, J., Thompson, G., Gillis, K., 1992. Lithium isotopic composition of submarine basalts: implications for the lithium cycle in the oceans. Earth Planet. Sci. Lett. 108, 151–160.

Chan, L.H., Leeman, W.P., You, C.F., 2002. Lithium isotopic composition of Central American volcanic arc lavas: implications for modification of subarc mantle by slab-derived fluids: correction. Chem. Geol. 182, 293–300.

Chan, L.H., Leeman, W.P., Plank, T., 2006. Lithium isotopic composition of marine sediments. Geochem. Geophys. Geosyst. 7, Q06005. doi:10.1029/2005GC001202.

Coogan, L.A., Kasemann, S.A., Charkraborty, S., 2005. Rate of hydrothermal cooling of new oceanic upper crust derived from lithium-geospeedometry. Earth Planet. Sci. Lett. 240, 415–424.

Crank, J., 1975. The Mathematics of Diffusion. Clarendon Press.

Decitre, S., Deloule, E., Reisberg, L., James, R., Agrinier, P., Mevel, C., 2002. Behavior of Li and its isotopes during serpentinization of oceanic peridotites. Geochem. Geophys. Geosyst. 3, 1007. doi:10.1029/2001GC000178.

Dick, H.J.B., Lin, J., Schouten, H., 2003. An ultraslow-spreading class of ocean ridge. Nature 426, 405–412.

Dodson, M.H., 1973. Closure Temperature in Cooling Geochronological and Petrological System. Contrib. Mineral. Petrol. 40, 259–274.

Dohmen, R., Kasemann, S.A., Coogan, L., Chakraborty, S., 2010. Diffusion of Li in olivine. Part I: experimental observations and a multi species diffusion model. Geochim. Cosmochim. Acta 74, 274–292.

Eggins, S.M., Rudnick, R.L., McDonough, W.F., 1998. The composition of peridotites and their minerals: a laser-ablation ICPMS study. Earth Planet. Sci. Lett. 154, 53–71.

Elliott, T., Jeffcoate, A., Bouman, C., 2004. The terrestrial Li isotope cycle: light-weight constraints on mantle convection. Earth Planet. Sci. Lett. 220, 231–245.

Elliott, T., Thomas, A., Jeffcoate, A., Niu, Y., 2006. Lithium isotope evidence for subduction-enriched mantle in the source of mid-ocean-ridge basalts. Nature (London) 443, 565–568.

Gallagher, K., Elliott, T., 2009. Fractionation of lithium isotopes in magmatic systems as a natural consequence of cooling. Earth Planet. Sci. Lett. 278, 286–296.

Gao, Y., Casey, J.F., in press. Lithium isotope composition of ultramafic geological reference materials: JP-1 and DTS-2. Geostand. Geoanal. Res. doi:10.1111/j.1751-908X.2011.00117.x.

Gao, Y., Huang, J., Casey, J.F., 2009. Data report: trace element geochemistry of oceanic crust formed at superfast-spreading ridge, Hole 1256D. In: Teagle, D.A.H., Alt, J.C., Umino, S., Miyashita, S., Banerjee, N.R., Wilson, D.S., Scientists, E. (Eds.), Proc. IODP, 309/312. Integrated Ocean Drilling Program Management International, Inc., Washington, DC. doi:10.2204/iodp.proc.309312.309202.302009.

Ionov, D.A., Seitz, H.M., 2008. Lithium abundances and isotopic compositions in mantle xenoliths from subduction and intra-plate settings: mantle sources vs. eruption histories. Earth Planet. Sci. Lett. 266, 316–331.

James, R.H., Palmer, M.R., 2000. The lithium isotope composition of international rock standards. Chem. Geol. 166, 319–326.

James, R.H., Allen, D.E., Seyfried, W.E., 2003. An experimental study of alteration of oceanic crust and terrigenous sediments at moderate temperatures (51 to 350 degrees C): insights as to chemical processes in near-shore ridge-flank hydrothermal systems. Geochim. Cosmochim. Acta 67, 681–691.

Jeffcoate, A.B., Elliott, T., Thomas, A., Bouman, C., 2004. Precise, small sample size determinations of lithium isotopic compositions of geological reference materials and modern seawater by MC-ICP-MS. Geostand. Geoanal. Res. 28, 161–172.
Jeffcoate, A.B., Elliott, T., Kasemann, S.A., Ionov, D., Cooper, K., Brooker, R., 2007. Li isotope fractionation in peridotites and mafic melts. Geochim. Cosmochim. Acta 71, 202–218.
Jokat, W., Ritzmann, O., Schmidt-Aursch, M.C., Drachev, S.S., Gauger, S., Snow, J.E., 2003. Geophysical evidence for reduced melt production on the Arctic ultraslow Gakkel mid-ocean ridge. Nature 423, 962–965.
Leeman, W.P., Tonarini, S., Chan, L.H., Borg, L.E., 2004. Boron and lithium isotopic variations in a hot subduction zone—the southern Washington Cascades. Chem. Geol. 212, 101–124.
Liu, C.Z., Snow, J.E., Hellebrand, E., Brügmann, G., von der Handt, A., Büchl, A., Hofmann, A.W., 2008. Ancient, highly heterogeneous mantle beneath Gakkel Ridge, Arctic Ocean. Nature 452, 311–316.
Lundstrom, C.C., Chaussidon, M., Hsui, A.T., Kelemen, P., Zimmerman, M., 2005. Observations of Li isotopic variations in the Trinity Ophiolite: evidence for isotopic fractionation by diffusion during mantle melting. Geochim. Cosmochim. Acta 69, 735–751.
Magna, T., Wiechert, U., Halliday, A.N., 2006. New constraints on the lithium isotope compositions of the Moon and terrestrial planets. Earth Planet. Sci. Lett. 243, 336–353.
Magna, T., Ionov, D.A., Oberli, F., Wiechert, U., 2008. Links between mantle metasomatism and lithium isotopes: evidence from glass-bearing and cryptically metasomatized xenoliths from Mongolia. Earth Planet. Sci. Lett. 276, 214–222.
Mallmann, G., O'Neill, H.S.C., Klemme, S., 2009. Heterogeneous distribution of phosphorus in olivine from otherwise well-equilibrated spinel peridotite xenoliths and its implications for the mantle geochemistry of lithium. Contrib. Mineral. Petrol. 158, 485–504.
Marschall, H.R., Altherr, R., Rüpke, L., 2007a. Squeezing out the slab — modelling the release of Li, Be and B during progressive high-pressure metamorphism. Chem. Geol. 239, 323–335.
Marschall, H.R., Pogge von Strandmann, P.A.E., Seitz, H.M., Elliott, T., Niu, Y., 2007b. The lithium isotopic composition of orogenic eclogites and deep subducted slabs. Earth Planet. Sci. Lett. 262, 563–580.
Michael, P.J., Langmuir, C.H., Dick, H.J.B., Snow, J.E., Goldstein, S.L., Graham, D.W., Lehnert, K., Kurras, G.J., Jokat, W., Mühe, R., Edmonds, H.N., 2003. Magmatic and amagmatic seafloor generation at the ultraslow-spreading Gakkel Ridge, Arctic Ocean. Nature 423, 956–961.
Ottolini, L., Le Fèvre, B., Vannucci, R., 2004. Direct assessment of mantle boronand lithium contents and distribution by SIMS analyses of peridotite minerals. Earth Planet. Sci. Lett. 228, 19–36.
Parkinson, I.J., Hammond, S.J., James, R.H., Rogers, N.W., 2007. High-temperature lithium isotope fractionation: insights from lithium isotope diffusion in magmatic systems. Earth Planet. Sci. Lett. 257, 609–621.
Peslier, A., Snow, J.E., Hellebrand, E., Von der Handt, A., 2007. Low water contents in Minerals from Gakkel ridge abyssal peridotites, Arctic Ocean. Geochim. Cosmochim. Acta 71, A779.
Phipps Morgan, J.P., Chen, Y.J., 1993. Dependence of ridge-axis morphology on magma supply and spreading rate. Nature 364, 706–708.
Richter, F.M., Davis, A.M., DePaolo, D.J., Watson, E.B., 2003. Isotope fractionation by chemical diffusion between molten basalt and rhyolite. Geochim. Cosmochim. Acta 67, 3905–3923.
Rieman, W., Walton, H.F., 1970. Ion Exchange in Analytical Chemistry. Pergamon Press Oxford, New York.
Rudnick, R.L., Ionov, D.A., 2007. Lithium elemental and isotopic disequilibrium in minerals from peridotite xenoliths from far-east Russia: product of recent melt/fluid–rock reaction. Earth Planet. Sci. Lett. 256, 278–293.
Rudnick, R.L., Nakamura, E., 2004. Preface to "Lithium isotope geochemistry". Chem. Geol. 212, 1–4.
Ryan, J.G., Kyle, P.R., 2004. Lithium abundance and lithium isotope variations in mantle sources: insights from intraplate volcanic rocks from Ross Island and Marie Byrd Land (Antarctica) and other oceanic islands. Chem. Geol. 212, 125–142.
Ryan, J.G., Langmuir, C.H., 1987. The systematics of lithium abundances in young volcanic rocks. Geochim. Cosmochim. Acta 51, 1727–1741.
Seitz, H.M., Woodland, A.B., 2000. The distribution of lithium inperidotitic and pyroxenitic mantle lithologies—an indicator of magmatic and metasomatic processes. Chem. Geol. 166, 47–64.
Seitz, H.M., Brey, G.P., Lahaye, Y., Durali, S., Weyer, S., 2004. Lithium isotopic signatures of peridotite xenoliths and isotopic fractionation at high temperature between olivine and pyroxenes. Chem. Geol. 212, 163–177.
Seyfried, W.E., Janecky, D.R., Mottl, M.J., 1984. Alteration of the oceanic crust: implications for geochemical cycles of lithium and boron. Geochim. Cosmochim. Acta 48, 557–569.
Seyfried, W.E., Chen, X., Chan, L.H., 1998. Trace element mobility and lithium isotope exchange during hydrothermal alteration of seafloor weathered basalt: an experimental study at 350 degrees C, 500 bars. Geochim. Cosmochim. Acta 62, 949–960.
Seyler, M., Lorand, J.P., Toplis, M.J., Godard, G., 2004. Asthenospheric metasomatism beneath the mid-ocean ridge: evidence from depleted abyssal peridotites. Geology (Boulder) 32, 301–304.
Shen, Y., Forsyth, D.W., 1995. Geochemical constraints on initial and final depths of melting beneath mid-ocean ridges. J. Geophys. Res. Solid Earth Planet. 100, 2211–2237.
Snow, J.E., Biegler, M., Eckardt, R., Feig, S., Feldmann, H., Gao, Y., Hellebrand, E., Janovic, T., Liesenfeld, T., Morgan, J., Nauret, F., Turini, S., Von de Handt, A., Weigler, K., 2007. Petrologic and tectonic evolution of the lena trough and western gakkel ridge. In: Budeus, G., Lemke, P. (Eds.), Cruise Report, Polarstern ARK XX-2: Reports on Polar and Marine Research. pp. 153–208.
Tang, Y.J., Zhang, H.F., Nakamura, E., Moriguti, T., Kobayashi, K., Ying, J.F., 2007. Lithium isotopic systematics of peridotite xenoliths from Hannuoba, North China Craton: implications for melt–rock interaction in the considerably thinned lithospheric mantle. Geochim. Cosmochim. Acta 71, 4327–4341.
Teng, F.Z., McDonough, W.F., Rudnick, R.L., Dalpe, C., Tomascak, P.B., Chappell, B.W., Gao, S., 2004. Lithium isotopic composition and concentration of the upper continental crust. Geochim. Cosmochim. Acta 68, 4167–4178.
Teng, F.Z., McDonough, W.F., Rudnick, R.L., Walker, R.J., 2006. Diffusion-driven extreme lithium isotopic fractionation in country rocks of the Tin Mountain pegmatite. Earth Planet. Sci. Lett. 243, 701–710.
Teng, F.Z., McDonough, W.F., Rudnick, R.L., Wing, B.A., 2007. Limited lithium isotopic fractionation during progressive metamorphic dehydration in metapelites: a case study from the Onawa contact aureole, Maine. Chem. Geol. 239, 1–12.
Tomascak, P.B., 2004. Developments in the understanding and application of lithium isotopes in the earth and planetary science. Rev. Mineral. Geochem. 55, 153–195.
Tomascak, P.B., Langmuir, C.H., 1999. Lithium isotope variability in MORB. EOS 80, F1086–F1087.
Tomascak, P., Widom, E., Benton, L., Goldstein, S., Ryan, J., 2002. The control of lithium budgets in island arcs. Earth Planet. Sci. Lett. 196, 227–238.
Tomascak, P.B., Langmuir, C.H., le Roux, P.J., Shirey, S.B., 2008. Lithium isotopes in global mid-ocean ridge basalts. Geochim. Cosmochim. Acta 72, 1626–1637.
Von de Handt, A., 2008. Deciphering Petrological Signatures of Cooling and Reactive Melt Stagnation at Ultraslow-spreading Ridges, Ph. D Thesis, Max-Planck Institute for Chemistry, Geochemistry / University of Mainz, Mainz, pp. 311.
Wunder, B., Meixner, A., Romer, R.L., Heinrich, W., 2006. Temperature-dependent isotopic fractionation of lithium between clinopyroxene and high-pressure hydrous fluids. Contrib. Mineral. Petrol. 151, 112–120.
Zack, T., Tomascak, P.B., Rudnick, R.L., Dalpe, C., McDonough, W.F., 2003. Extremely light Li in orogenic eclogites: the role of isotope fractionation during dehydration in subducted oceanic crust. Earth Planet. Sci. Lett. 208, 279–290.